A Theoretical Study of Propagation Rate Coefficients for Methacrylonitrile and Acrylonitrile

David M. Huang, Michael J. Monteiro, and Robert G. Gilbert*

School of Chemistry, University of Sydney, New South Wales 2006, Australia

Received February 13, 1998; Revised Manuscript Received June 5, 1998

ABSTRACT: The propagation rate coefficients for methacrylonitrile (MAN) and acrylonitrile (AN) were calculated using transition state theory and high-level ab initio molecular orbital theory. The calculations take particular account of internal rotations in the transition states. Frequency factors and rotational potentials were found to be insensitive to the level of theory used (except that the semiempirical AM1 method does not perform very well), because of cancellations in the partition function ratio in transition state theory; however, two of the internal rotations studied were found to be sensitive to the chain length of the radical used in the calculations. Activation energies were found to be extremely sensitive to the level of theory. At the highest level of theory used, the calculated frequency factor for MAN was slightly lower than experiment, while the activation energy was 2.6 kJ mol^{-1} higher than experiment. Theoretical comparison of propagation of MAN and AN was used to explain differences observed experimentally in activation energies and frequency factors of methacrylates and corresponding acrylates. The higher frequency factors for methacrylates are largely due to hindrance caused by the methyl groups to the three transitional modes in the transition state which correspond to the three external rotational degrees of freedom of the monomer in the reactants (but not a result of increased hindrance to methyl rotation itself in the transition state). The higher activation energies of methacrylates arises from differences in hindrance and loss of delocalization in the transition states of the methyl-substituted and unsubstituted monomers.

Introduction

Many fundamental aspects of free-radical polymerization are still poorly understood. Theory can provide valuable insights into trends and also can make qualitative and quantitative estimates of the propagation rates for monomers for which the rate coefficient has not been experimentally measured. The advent of pulsed laser polymerization (PLP) has allowed the accurate measurement of frequency factors and activation energies for propagation reactions,[1−5] which in turn provides the opportunity to test theoretical models against experiment.

The aims of this work are 2-fold: first, to test a means for calculating rate coefficients using transition state theory (TST) and ab initio molecular orbital (MO) theory for propagation of a substituted monomer (methacrylonitrile, MAN) and, second, to compare propagation of two different monomers (MAN and acrylonitrile, AN), to explain general trends observed in frequency factors and activation energies. The only previous work to use high level ab initio calculations is on the propagation of ethylene,[6−8] for which the experimental data at ambient pressure are not very accurate; however, PLP data of acceptable accuracy are available for MAN.[9] Substituted monomer systems present a number of challenges not encountered with ethylene. The availability of accurate experimental Arrhenius parameters for MAN enables a proper test of the present theoretical approach. The method used here ignores the effect of solvent; provided the transition state and quantum calculations are of sufficiently high accuracy, comparison between theory and experiment should then give some indication of the importance of solvent effects. The study of the polymerization of substituted monomers may also reveal interesting features not encountered with ethylene. The MAN/AN comparison (methyl-substituted vs unsubstituted monomer) can be used to explain systematic differences such as those in frequency factors (A) and activation energies (E_a) for propagation of butyl methacrylate (BMA) and butyl acrylate (BA): PLP measurements have found that A for BA is $\sim$ 7 times larger than for BMA, while E_a for BA is $\sim$ 4.4 kJ mol^{-1} lower than for BMA, trends also seen for other acrylate/methacrylate systems.[10−13] Another seemingly general observation is that frequency factors and activation energies for homopropagation in homologous series (e.g., in all extant data on methacrylate k_p's,[11,14] and again in vinyl acetate vs vinyl *neo*decanoate[15−17]) are very similar but show small systematic differences. A general explanation for such trends is useful, even in an industrial context: for example, it is important to know if all acrylates are likely to propagate extremely quickly and that this high rate will be only weakly affected by temperature (i.e., the propagation reaction has a low E_a), while the situation with methacrylates is correspondingly different.

Transition State Theory and Quantum Procedures

The rate coefficient for a bimolecular reaction in transition state theory (TST) is given by (e.g.,[18])

$$k = \frac{m^{\dagger}\sigma}{m\sigma^{\dagger}} \frac{k_B T}{h} \frac{Q^{\dagger}}{Q_A Q_B} \exp(-E_0/k_B T) \qquad (1)$$

where k_B is the Boltzmann constant, T is the temperature, Q_A, Q_B, and $Q^{\dagger}$ are the partition functions for reactant A, reactant B, and the transition state (TS) respectively, E_0 is the energy difference between the

* To whom correspondence should be addressed.

S0024-9297(98)00229-0 CCC: $15.00
Published on Web 07/22/1998

zero-point vibrational energy levels of the reactants, and TS, and σ ($\sigma^\dagger$), and m ($m^\dagger$) are the symmetry numbers and numbers of optical isomers of reactant (transition state). Assuming separability of the molecular Hamiltonian, the partition function Q can be written as a product of translational, vibrational, and rotational terms. Because in a propagation reaction, one of the reactants (the propagating chain) and the TS are both very heavy, the ratio of translational partition functions (per unit volume) reduces to[6]

$$\left.\frac{Q^\dagger}{Q_A Q_B}\right|_{\text{trans}} = \left(\frac{h^2}{2\pi M_0 k_B T}\right)^{3/2} \tag{2}$$

where M_0 is the molecular weight of a monomer unit. The vibrational partition functions are given by $[1 - \exp(-h\nu/k_B T)]^{-1}$ for a harmonic oscillator of frequency ν; there is one less degree of freedom in the transition state than in reactants. Because of the heavy mass of the chain, the external rotational partition function ratio for a polymer propagation is given by

$$\left.\frac{Q^\dagger}{Q_A Q_B}\right|_{\text{rot}} = \pi^{-1/2}\left(\frac{8\pi^2 k_B T I_a I_b I_c}{h^2}\right)^{-3/2} \tag{3}$$

where I_a etc. are the principal moments of inertia of monomer. It is essential to take into account the internal rotational part of the partition functions: many low-frequency modes are in fact hindered rotors. Partition functions for these modes are found from the energy levels obtained by numerically solving the one-dimensional rotational Schrödinger equation for the rotational potential corresponding to that mode.[6] The activation energy and frequency factor are found by numerical differentiation (second-order finite difference for temperatures a few kelvin either side of the desired temperature, the activation energy being only very weakly temperature-dependent):

$$E_a = -\frac{\partial(\ln k)}{\partial(1/k_B T)}; \quad A = k \exp(E_a/k_B T) \tag{4}$$

It is noted that because the TS expression contains a ratio of partition functions, one has essentially exact cancellation of many effects such as large-scale internal rotational modes of the polymer chain.[6]

Conventional TST, as it is applied in the present work, possesses several limitations (e.g., see refs 19 and 20). These include neglect of anharmonicity (for modes treated as harmonic oscillators; it has been established[18] that this neglect is unimportant in TST for modes that are not hindered rotors), the assumption of a separable reaction coordinate, neglect of recrossing of the TS surface, and neglect of solvent effects (the present calculations assume gas-phase reactions). The errors due to these approximations may not be too severe in calculations on propagation reactions, which have sharp barriers and involve two "large" reactants, so recrossing[21] and solvent "friction" at the TS[22] may not be important. The TSs also do not involve significant charge transfer, so the effect of solvent polarity on E_a is likely to be small.

Geometries were optimized and harmonic vibrational frequencies and energies calculated using standard ab initio molecular orbital procedures.[23] These calculations were carried out at the AM1, UHF/3-21G, UHF/6-31G*, and UB3-LYP/6-31G* levels of theory for MAN and at the UHF/6-31G* level for AN. Although one cannot expect accuracy from the semiempirical AM1 method, preliminary calculations using this technique often give a useful first estimate of geometry which can be used as a starting point for calculations using adequate levels of theory. Energies were calculated up to the UQCISD/6-31G* level of theory. Heuts *et al.*[7] suggest that the UHF/6-31G* level is adequate for the calculation of frequency factors (based on work on propagation of ethylene) while much higher levels (at least QCISD(T)/6-311G**) are required for energies.

Some low-frequency vibrations (<200 cm^{-1}) were treated explicitly as internal rotations, since these modes are not only significantly anharmonic but also make major contributions to the partition functions. These internal rotations were identified by computer-animating the normal modes; rotational potentials were then calculated by fully optimizing the geometries at a number of points along the rotational coordinate and fitting to a piecewise smooth cubic spline. The reduced moments of inertia for these modes were found from the moments of inertia of the counter-rotating moieties about the appropriate axis. For calculations using UHF/6-31G* geometries, rotational potentials were calculated at the UHF/6-31G* level or at the UHF/3-21G level if these were not available (it will be shown later that the lower level of theory gives almost identical rotational potentials as the higher level; while high-level theory is required to calculate activation energies, it has been shown[6] that rotational potentials are much less sensitive to the level of theory because they are strongly influenced by geometrical considerations, which require much less accurate accounting for electron correlation).

All other modes were treated as harmonic oscillators. This approximation is certainly not accurate as far as individual partition functions are concerned. However, the approximation is in fact quite sufficient to calculate the frequency factor with acceptable accuracy, as shown by the observation (both in the present calculations and elsewhere[6,8]) that the calculated value of A is insensitive to the level of quantum theory used. The reason for this is that effects of anharmonicities in corresponding modes approximately cancel in $Q^\dagger/Q$, to which A is approximately proportional. Anharmonicity also has a small effect on the activation energy, through the difference in zero-point energies of reactant and transition state; anharmonicities are only significant in low-frequency modes and thus have negligible effect on the difference of zero-point energies.

To simulate the long polymer chain, the hydrogen atom shown in Figure 1 in the radical and TS was replaced by a large mass (arbitrarily chosen as 9999). Harmonic frequencies were recalculated for these "macroradicals" using the same force constants as for the short chain species. Earlier work[6] has shown that this is adequate for obtaining partition functions for both harmonic and hindered-rotor modes, provided that the heavy atom is put at the far end of the dimeric radical in a dimeric-radical/monomer reactant/transition-state system: that is, doing nothing more than putting a heavy atom at the end (which affects only the G matrix in a normal mode calculation and the moment of inertia in a calculation of a hindered-rotor partition function) of such a "trimer" gives all the information that is necessary to find $Q^\dagger/Q$ with adequate accuracy. All frequencies and zero-point energies were multiplied by empirical scaling factors (low-frequency scale factors

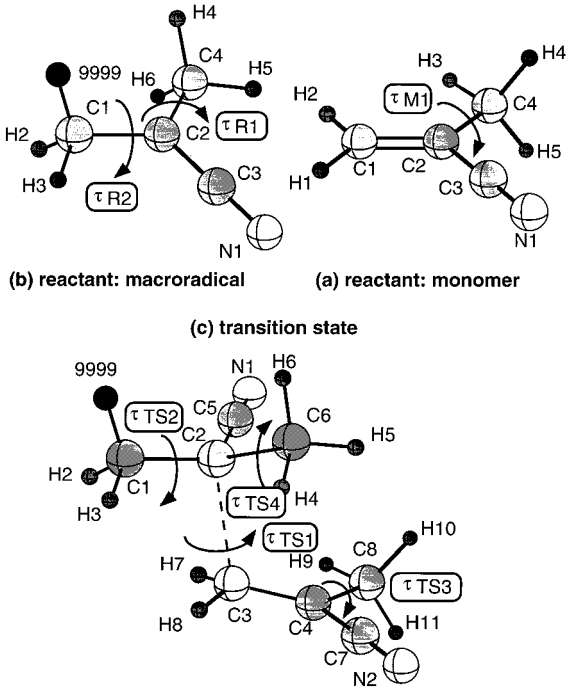

Figure 1. Schematic representation of MAN (a) monomer (b) (macro-) radical, and (c) syndiotactic dimer TS showing internal rotations.

used at all levels of theory except UHF/6-31G*, where high and low-frequency scale factors are almost identical).[24]

All ab initio MO theory calculations were carried out with the GAUSSIAN 94 software package.[25]

Results and Discussion

Geometries considered were those of the MAN and AN monomers, monomer and dimer radicals, syndiotactic and isotactic dimer TSs, and the "*rr*" trimer TS. This last is one of the eight stereoisomers of the MAN trimer transition state, which are named with the diad nomenclature: if identical substituents in adjacent monomer units on the chain are on opposite sides of the plane, the diad is referred to as racemic (*r*). Geometries were optimized at various levels of theory. The geometries and internal rotations of the MAN monomer, radical and syndiotactic dimer TS are shown in Figure 1 (internal rotations are denoted by τ). All normal-mode frequencies below 200 cm^{-1} of the MAN and AN monomers, syndiotactic dimer radicals and *rr* trimer TSs and the assigned internal rotations are given in Table 1. In AN, only τ_{R1}, τ_{TS1}, and τ_{TS2} are present. Rotational potentials were calculated for all of these modes.

Table 2 shows these frequencies re-grouped so that approximate matchings have been assigned to corresponding modes in reactant and transition state, and in MAN and AN (of course, these matchings are not exact); matching was through similar dynamics as seen in the animations of the modes. Some of these modes are internal rotations, discussed immediately below, and these or others can also sometimes be "transitional modes",[18] which are modes which are free rotations and translations of monomer in the reactant configuration but internal modes in the transition state. Thus, taking ethylene propagation as a simple example, the free rotation of ethylene monomer in the plane in the reactant configuration becomes a torsion (hindered rotor) in the transition state.

Table 1. Normal Mode Frequencies (cm^{-1}) under 200 cm^{-1} in MAN and AN Monomer, Syndiotactic Dimer Radical, and *rr* Trimer TS and Assignment of Modes to Internal Rotations (Scaled Macroradical Frequencies Used)

		MAN		AN	
species	mode	frequency	assignment	frequency	assignment
monomer	ν_1	167	τ_{M1}		
	ν_2	193			
syn dimer radical	ν_1	29	τ_{R1}	19	τ_{R1}
	ν_2	53		50	
	ν_3	69	τ_{R2}	73	
	ν_4	76		128	
	ν_5	103		160	
	ν_6	124		183	
	ν_7	142			
	ν_8	177			
rr trimer TS	ν_1	503i		444i	
	ν_2	16	τ_{TS1}	18	τ_{TS1}
	ν_3	30	τ_{TS2}	25	τ_{TS2}
	ν_4	50		44	
	ν_5	59		55	
	ν_6	73		69	
	ν_7	80		76	
	ν_8	99	τ_{TS3}	96	
	ν_9	102		134	
	ν_{10}	113		156	
	ν_{11}	127		206	
	ν_{12}	161			
	ν_{13}	169			
	ν_{14}	184			
	ν_{15}	204			
	ν_{16}	223	τ_{TS4}		

Internal Rotations. Because the (hindered) internal rotational modes have a strong effect on the frequency factor, and, as will be seen later, also influence the activation energy, they must be treated in considerable detail.

The rotational potentials for τ_{M1}, τ_{R1}, τ_{R2}, τ_{TS1}, τ_{TS2}, τ_{TS3}, and τ_{TS4} are given in Figures 2−8, respectively. All potentials were calculated using monomer, monomer radical and dimer TS except for τ_{R1} and τ_{TS2}, which were calculated using the dimer radical and trimer TS. There are a large number of low frequencies in the radicals and TSs (12 frequencies less than 200 cm^{-1} in the MAN syndiotactic dimer TS), most of which could not be ascribed to any simple motion. These were treated as harmonic oscillators.

The relatively low levels of theory used for the treatment of the partition functions of internal rotations (the highest level used for the optimization was UHF/6-31G*) appear to be adequate (although activation energies are very sensitive to the level of theory used). Moments of inertia were found to be unaffected by the level of theory used (variation <10%), since geometries are relatively insensitive to the level of theory. Rotational potentials also appear to change only slightly at different levels of theory, as shown for τ_{TS1} in Figure 9. Even the relatively computationally inexpensive UHF/3-21G level of theory gives rotational barriers similar to those obtained from much higher levels of theory for all of the rotations. The barrier to rotation for τ_{TS2} was calculated at the UHF/6-31G* level using the UHF/3-21G geometries of the stationary points and found to be 11.3 kJ mol^{-1} (virtually identical to the UHF/3-21G results). A similar calculation for τ_{TS4} gave barriers of 11.1 and 11.9 kJ mol^{-1} respectively at the UHF/3-21G and UHF/6-31G* levels. This suggests that the UHF

Table 2. Lower Frequencies (cm^{-1}) of Reactant and Transition State for MAN and AN, Where Each Reactant Mode Has Been Associated with a Corresponding Transition State Mode

TS Mode	MAN	MAN†	assignment	AN	AN†	assignment
ν_1		503i	transitional (trans)		444i	transitional (trans)
ν_2		16	τ_{TS1} transitional (rot)		18	τ_{TS1} transitional (rot)
ν_3	29	30	τ_{R1}/τ_{TS2}		25	τ_{R1}/τ_{TS2}
ν_4	53	50	ν_2 (rad)	50	44	ν_2 (rad)
ν_5		59	transitional (rot)		55	transitional (rot)
ν_6		73	transitional (trans)		69	transitional (trans)
ν_7	76	80	ν_4 (rad)	73	76	ν_3 (rad)
ν_8	177	99	τ_{M1}/τ_{TS3}		96	transitional (rot)
ν_9	103	102	ν_5 (rad)	128	134	ν_4 (rad)
ν_{10}		113	transitional (rot)	161	156	ν_5 (rad)
ν_{11}	124	127	ν_6 (rad)	183	206	ν_6 (rad)
ν_{12}	142	161	ν_7 (rad)			
ν_{13}	284	169	ν_3 (mon)			
ν_{14}	177	184	ν_8 (rad)			
ν_{15}	193	204	ν_2 (mon)			
ν_{16}	69	223	τ_{R2}/τ_{TS4}			

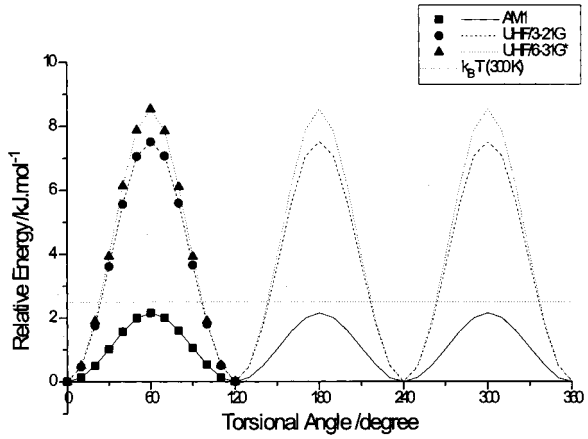

Figure 2. Rotational potential for τ_{M1} (methyl rotation) in MAN monomer, as a function of dihedral angle d(H3−C4−C2−C1) defined in Figure 1a. Broken line in this and subsequent figures is k_BT (thermal energy at 300 K).

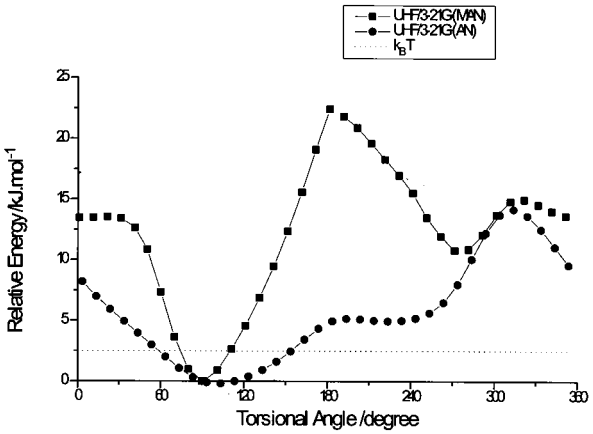

Figure 3. Rotational potential for τ_{R1} in MAN and AN dimer radical as a function of dihedral angle d(C5−C4−C3−C2) defined in Figure 1c. Note that the apparent discontinuity in curve for MAN does not affect Q because the discontinuity is well above k_BT.

level of theory is adequate for calculating rotational barriers. Previous calculations have also found that rotational barriers do not change significantly with the level of theory used.[23,26] This is what one would expect, since rotations do not involve bond formation or breaking, which is where the inadequacies of methods using single configurational wave functions (e.g. UHF) most clearly manifest themselves. Comparison between the UHF/3-21G and UHF/6-31G* potentials can also be

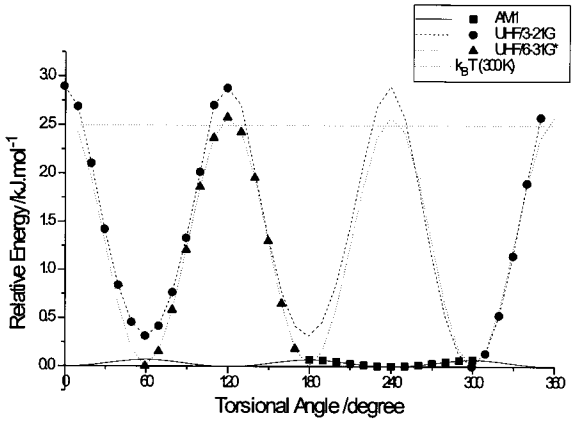

Figure 4. Rotational potential for τ_{R2} (methyl rotation) in MAN monomer radical as a function of dihedral angle d(H4−C4−C2−C3) defined in Figure 1b.

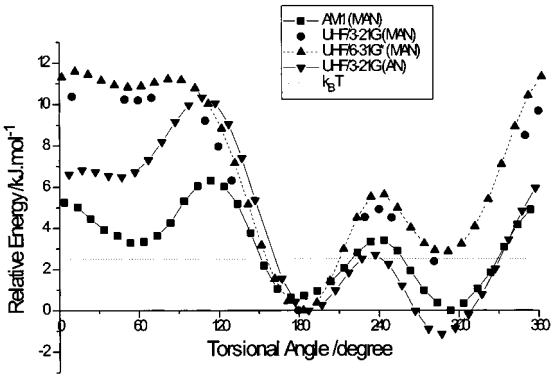

Figure 5. Rotational potential for τ_{TS1} in MAN and AN syndiotactic dimer TSs as a function of dihedral angle d(C1−C2−C3−C4) defined in Figure 1c.

justified due to their similarity (calculations at the UHF/6-31G* level were sometimes not carried out due to the computational expense of such calculations). However, it is obvious from Figures 2−8 that the semiempirical AM1 method underestimates all of the rotational barriers. Such underprediction has been seen elsewhere for closed-shell systems,[27−29] although in the present case the underprediction is more pronounced for radical systems.

The rotational potentials for τ_{R1} and τ_{TS2} were calculated using the dimer radical and trimer TS respectively, while the potentials for all other rotations were only treated using the monomer radical and dimer TS. This is because it has been shown previously for

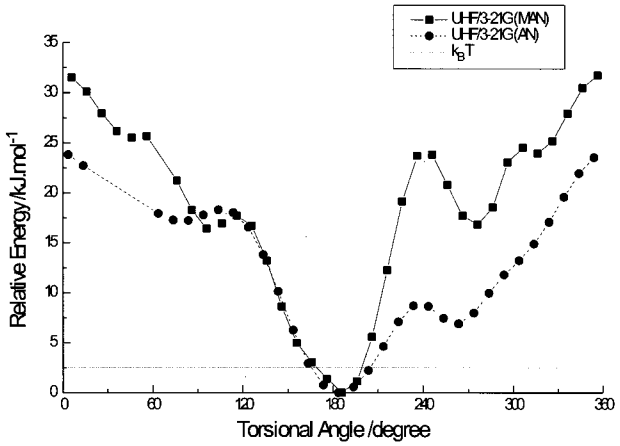

Figure 6. Rotational potential for τ_{TS2} in MAN and AN *rr* trimer TSs as a function of dihedral angle *d*(C5−C4−C3−C2) defined in Figure 1c.

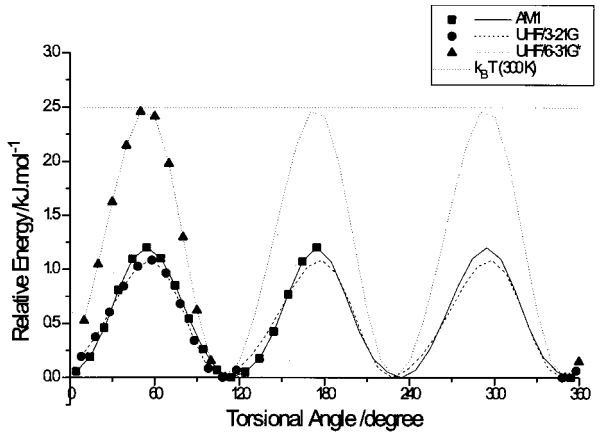

Figure 7. Rotational potential for τ_{TS3} (monomer CH_3 rotation) in MAN syndiotactic dimer TS (as a function of dihedral angle *d*(H9−C8−C4−C3) defined in Figure 1c.

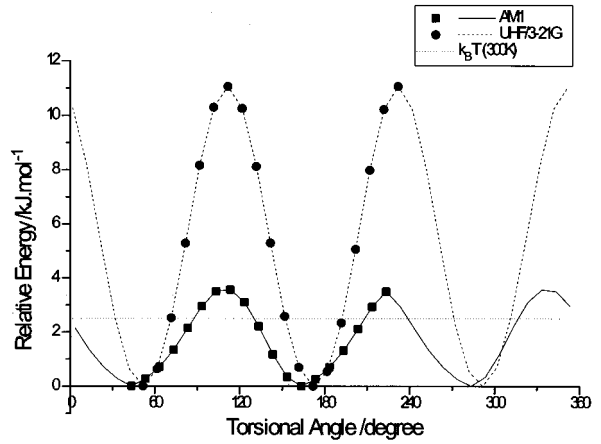

Figure 8. Rotational potential for τ_{TS4} (radical CH_3 rotation) in MAN syndiotactic dimer TS (as a function of dihedral angle *d*(H4−C6−C2−C1) defined in Figure 1c.

ethylene[7,26] that the τ_{R1} and τ_{TS2} rotations are significantly affected by the chain length of the radical used in the calculations. The changes to these rotational potentials in MAN were found to be greater than those in ethylene. In changing from the monomer to dimer radicals, the barrier to the τ_{R1} rotation at the UHF level changes from 2.5 kJ mol^{-1} to 15 kJ mol^{-1} (Figure 3). For comparison, the corresponding barrier height in calculations on ethylene[7,26] changed very slightly (from

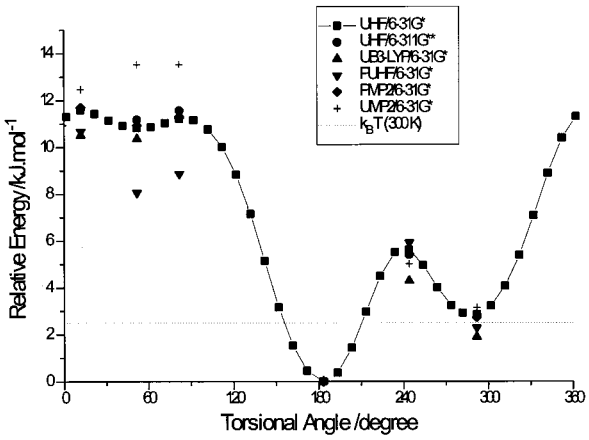

Figure 9. Rotational potentials for τ_{TS1} calculated at various levels of theory using UHF/6-31G* geometries.

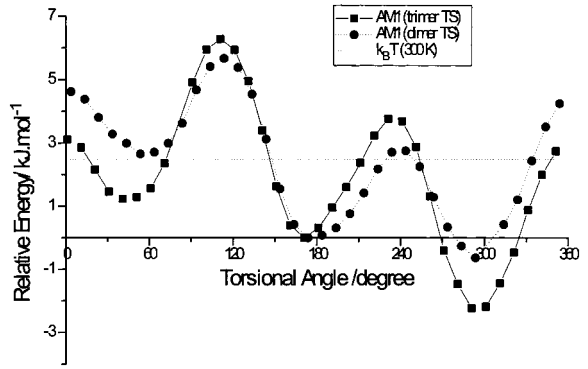

Figure 10. Rotational potential for τ_{TS1} in MAN syndiotactic dimer and *rr* trimer TS at AM1 level of theory.

0.6 to 1.2 kJ mol^{-1}) with the same levels of theory. In changing from the dimer to trimer TS, the barrier to the τ_{TS2} rotation at the UHF level changes from 11 to 32 kJ mol^{-1} (Figure 6). On the other hand, Figure 10, which gives the AM1 rotational potential for τ_{TS1} for the *rr* trimer transition state and syndiotactic dimer TS, shows that this mode is unaffected by chain length (this comparison using the lowest level of theory is meaningful because while AM1 does not give absolute energies with useful accuracy, it is seen that the hindered-rotor potential curves are semiquantitatively similar at all levels of theory). This is because steric hindrance to rotation in this mode is not affected very much by parts of the chain more than two carbon atoms from the axis of rotation. Therefore, while the τ_{TS1} rotation is adequately treated with the dimer transition state, the τ_{R1} and τ_{TS2} rotational potentials need to be calculated using at least the dimer radical and trimer transition state, respectively. Although rotational potentials are affected by chain length, moments of inertia for all internal rotations were found to be unchanged by the chain length of the radical used for all rotations.

Table 3 lists the partition functions for the MAN internal rotations calculated using the UHF/6-31G* rotational potentials, the partition functions calculated using the scaled UHF/6-31G* harmonic frequencies for these modes, and the free rotor partition functions calculated using the UHF/6-31G* reduced moments of inertia. The partition functions in Table 3 show that the *Q*'s for the methyl rotations τ_{M1}, τ_{R2}, τ_{TS3}, and τ_{TS4} can all be treated adequately as harmonic oscillators. The partition function for τ_{TS3} is also adequately approximated as that for a free rotation (note that Figure

Table 3. Comparison of Internal Rotational Partition Functions, Harmonic Oscillator Partition Functions, and Free Rotor Partition Functions for MAN Internal Rotations (Calculated at 303 K)

mode	$Q_{\text{int rot}}$	Q_{harmonic}	$Q_{\text{free rot}}$
τ_{M1}	1.92	1.82	3.60
τ_{R1}	7.38	7.75	22.5
τ_{R2}	2.96	3.57	3.64
τ_{TS1}	24.3	14.0	115
τ_{TS2}	13.4	7.58	159
τ_{TS3}	3.00	2.66	3.64
τ_{TS4}	1.66	1.53	3.64

7 suggests that while the partition function for this mode can by numerical coincidence be adequately treated as either free rotor or harmonic oscillator, a free rotor is the best interpretation); τ_{R1} also appears to be a harmonic oscillator. None of these results are surprising in view of the type of mode. These results can be used to reduce the computational expense of future calculations by avoiding time-consuming rotational potential scans. The last two internal rotations, τ_{TS1} and τ_{TS2}, cannot however be adequately treated as either harmonic oscillators or free rotors. This is clearly illustrated for τ_{TS1} in Figure 5 in which two valleys in the potential energy surface are thermally accessible from the potential minimum (so it is not a harmonic oscillator) while parts of the surface lie well above k_BT (so it is not a free rotor). For τ_{TS2} (Figure 6), only one valley in the potential energy surface is thermally accessible. However, this mode is not harmonic because the surface is not parabolic. Since the reduced moment of inertia for this mode is quite large, there is a large number of energy levels below 200 cm^{-1} which contribute significantly to the partition function. These energy levels are quite different for the calculated hinder-rotor potential and for the harmonic approximation, resulting in a large difference in $Q_{\text{int rot}}$ and Q_{harmonic}.

Calculation of k_p. The value of k_p was calculated using eq 1 for the reaction monomer + monomer radical → dimer radical TS, and monomer + syndiotactic dimer radical → *rr* trimer radical TS. For MAN, the translational and external rotational partition functions show little variation with the level of theory used. However, the vibrational partition functions vary widely, due to small nonsystematic differences in the large number of low frequencies in the TS. The frequency factor was not calculated at the AM1 level of theory because this often gave two imaginary frequencies for the monomer radical. Critical energies (and hence E_a) vary widely with level of theory and number of monomeric units; the level at which "chemical" accuracy can be obtained for E_a has been discussed elsewhere.[6,7]

The reaction path degeneracy factor $m^{\dagger}\sigma/m\sigma^{\dagger}$ in eq 1 was 2, since each TS exists as a pair of enantiomers. The value of k_p for the formation of the syndiotactic TS must also be added to that for the isotactic TS. It will be shown later that E_a for isotactic addition is much higher than E_a for syndiotactic addition at all levels of theory, and so only the syndiotactic addition is considered in comparison of the calculated k_p with experiment.

Comparison with Experiment

Experimental Arrhenius parameters for MAN are shown in Figure 11, as the 95% joint confidence intervals recalculated (using the method of van Herk[30]) from the experimental k_p values reported by Shipp et al.[9] at different temperatures. The uncertainty in k_p for all of the experimental data points, needed to determine the confidence interval, was assumed to be 20%. This is based on the difference between literature values of intrinsic viscosity and recent triple-detector size-exclusion chromatography (TD−SEC) results measured by Hutchinson *et al.*,[17] found to range from 10 to 20% for most monomers. This translates to an error in molecular weight of ∼20%. Also given in Figure 11 are the calculated Arrhenius parameters (*A* calculated with either τ_{TS1} and CH_3 rotations or all internal rotations for the formation of the *rr* trimer TS and E_a calculated at QCISD/6-31G* level of theory).

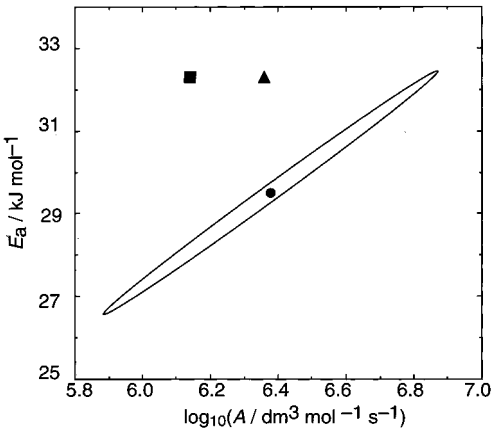

Figure 11. Line and point (●): 95% joint confidence interval for experimentally measured Arrhenius parameters for k_p of MAN compared with theoretical results, the center point (●) being the best-fit value. Other points are theory: *A* calculated with τ_{TS1} and CH_3 rotations (■), or all internal rotations (▲). E_a was calculated at the QCISD/6-31G* level of theory.

In addition to uncertainty arising from experimental scatter, there are also some questions about systematic errors in the experiments used to measure k_p by PLP,[9] since the Mark−Houwink parameters (*K* and *a*) used to calibrate the molecular weight distribution measured by GPC may be incorrect. The *K* and *a* values for MAN were not measured using the recommended[4,17] method of triple-detector size-exclusion chromatography (TD−SEC). Instead, they were measured using viscometry in DMF with Ubbelohde viscometers and calibration was carried out using literature *K* and *a* values determined in acetone by viscometry. Work is currently under way to measure *K* and *a* values for MAN by TD−SEC for reprocessing of the PLP data.

Experimental and Calculated Frequency Factors. The calculated frequency factors for MAN and AN are given in Table 4, showing that while experiment and theory are generally close, the theoretical results are almost always lower than experiment. The value of *A* for MAN calculated at the UHF/6-31G* level of theory with the *rr* trimer TS, which includes the partition function for τ_{TS1} and CH_3 rotations, is a factor of 2 smaller than the experimental value. The value of *A*, which also includes the τ_{R1} and τ_{TS2} internal rotations, agrees quite acceptably with experiment. This final result must however be treated with some caution, since the normal modes that were replaced by these internal rotations did not correspond to pure 1-dimensional τ_{R1} and τ_{TS2} rotations. In contrast, the normal modes that were replaced by the τ_{TS1} and CH_3 rotations were clearly simple 1-dimensional rotations.

The calculations show that the frequency factor increases with chain length. The increase from dimer to trimer is because the τ_{R1} internal rotation is much

Table 4. Frequency Factors for Propagation of MAN and AN

type of TS	level of theory	int rotors	log (A/M^{-1}·s-1) MAN	log (A/M^{-1}·s-1) AN	$A_{AN/AMAN}$
syndiotactic dimer	UHF/3-21G		5.53		
	UHF/3-21G	τ_{TS1}	5.97		
	UB3-LYP/6-31G*		5.59		
	UHF/6-31G*		5.34	5.68	2.2
	UHF/6-31G*	τ_{TS1}	5.87	6.30	2.7
	UHF/6-31G*	τ_{TS1} + CH_3 rotations	5.96	6.30	2.2
rr trimer	UHF/6-31G*		5.54	6.30	6.0
	UHF/6-31G*	τ_{TS1}	5.96	6.81	7.1
	UHF/6-31G*	τ_{TS1} + CH_3 rotations	6.14	6.81	4.7
	UHF/6-31G*	all	6.36	6.83	2.9
experiment			6.43 ± 0.26		

looser in the dimer radical than in the monomer radical. Previous work on ethylene[7,26] found that the frequency factor for the trimer and TSs up to nine carbon atoms in length were within a factor of 1.6 of each other, and therefore the above treatment for the MAN trimeric system is probably adequate.

The calculations show that A is fairly insensitive to the three different levels of theory used. The frequency factors calculated for the dimer TS using only harmonic frequencies lie within a factor of 1.8 of each other. The UHF/3-21G and UHF/6-31G* calculations which include the τ_{TS1} internal rotation only differ by 26%. The UB3-LYP/6-31G* frequency factor is larger than the others because the TS optimized at this level of theory was found to be more "loose" than at the other levels (the forming C−C bond length is 2.27 Å with UB3-LYP/6-31G* compared to 2.19 Å with UHF/6-31G*), resulting in lower frequencies in the TS than at the other levels of theory (this was also observed with calculations on the propagation of ethylene[7,26]).

There is a relatively small discrepancy between the frequency factors deduced from experiment and found here by calculation: if the uncertainties in the experimental values are included, the theoretical value is within 7% of the 95% confidence interval (Figure 11). One reason may be uncertainties or errors in the experimental result, discussed above. Another possible reason for the small discrepancy could be due to solvent effects. One way in which solvent may act is by providing a "frictional" force[22,31,32] to the external rotation of the monomer. This effectively provides a barrier to rotation, reducing the monomer partition function and thus increasing the calculated value of k_p: i.e., this would increase the calculated A factor, a hypothesis in accord with the observation that the (gas-phase) A factors calculated here appear to be systematically smaller than experiment. The fact that the present calculations yield results that are at worst no more than a factor of 2 different from experiment suggests that indeed such solvent effects are small.

A third possible explanation for the small discrepancy in A between theory and experiment is that this is due to the accumulation of a small error (e.g., 10%) in the partition function ratios ($Q^{\dagger}/Q$) for a large number of low frequency (or rotationally hindered) modes, especially for those which are slightly different between reactant and transition state and involve more than the three monomer units considered here.[6]

Experimental and Calculated Activation Energies. E_a was calculated at a number of different levels of theory using the UHF/6-31G* geometries. This is summarized in Table 5, which shows a huge variation in the calculated E_a's. This scatter in E_a has been observed in other calculations for radical reactions.[7,8,26,33] The highest level of theory used, QCISD/6-31G*, gives an activation energy for MAN quite close to the experimental value, although the result may be fortuitous, as this level of theory is not as good as the lowest level recommended for such calculations (QCISD(T)/6-311G**).[8] The MAN system is also very badly affected by spin contamination ($\langle S^2 \rangle = 1.21$ in the TS compared with 0.75 for a pure doublet), which can result in errors in UMP energies.[34−36]

One interesting feature in Table 5 is that the difference in E_a between the isotactic and syndiotactic dimer transition states is roughly unchanged between all levels of theory, being approximately 10 and 8 kJ mol^{-1} respectively for MAN and AN. The difference in E_a is probably independent of theory because the stereoisomeric TSs differ mainly in the degree of bond-bending and nonbonded interactions. The energetics of such interactions are adequately described by low levels of theory (e.g. no bonds formed/broken, and the energy bond-bending is independent of level of theory, as evident from the similarities between harmonic frequencies calculated at different levels). If this difference is real (which the consistency of the difference at all levels of theory appears to show), it indicates that reaction via the syndiotactic pathway occurs ~97% of the time at 80 °C and so isotactic addition can be ignored.

Trends in Frequency Factors. The acceptable accord for experimental frequency factors, and perhaps for activation energies, at the highest level of theory used here suggests that this is an adequate simulation of the electronic structure for the differences between reactant and transition state. It is highly likely that the simulations can be used for an analysis of trends, since any differences between reality and our quantum calculations should be similar for each member in a series of homologous reactions. Such trends are, for example, the observation (which is likely to be general) that acrylates have lower activation energies and higher frequency factors than the corresponding methacrylates.

The value of A for AN calculated at the UHF/6-31G* level of theory with the *rr* trimer TS is 4.7 times that for MAN (when the partition function for τ_{TS1} and CH_3 rotations are included—see Table 4). When the partition function for the τ_{R1} and τ_{TS2} rotations are included, the difference is reduced to a factor of 2.8, although as discussed before this must be treated with some degree of caution. Given this caveat, the theoretical results for MAN/AN are in agreement with the experimental trend for BMA/BA and other acrylate/methacrylate systems.

While eqs 1 and 4 (the latter in fact defining the activation energy and frequency factor in terms of the

Table 5. Activation Energies (kJ mol^{-1}) for Propagation of MAN and AN (for Dimer TS), Where the Level of Theory Approximately Increases in Accuracy down the Table

	MAN			AN			
level of theory[a]	syn[b]	iso[c]	ΔE_a[d]	syn[b]	iso[c]	ΔE_a[d]	MAN−AN[e]
UHF/3-21G	36.2						
UHF/6-31G*	56.1	67.0	10.9	49.3	56.9	7.6	6.7
UHF/6-31G**	56.8						
UHF/6-311G**	60.9						
UMP2/6-31G*	50.8	64.1	13.4	63.4	72.9	9.5	−12.6
UMP2/6-311G**	45.5						
UMP3/6-31G*	55.7	68.3	12.6	63.5	72.2	8.7	−7.8
UMP3/6-311G**	51.5						
UMP4(D)/6-31G*	56.6	69.1	12.5	65.4	74.0	8.6	−8.7
UMP4(D)/6-311G**							
UMP4(DQ)/6-31G*	55.9	68.2	12.3	63.8	72.4	8.6	−7.9
UMP4(DQ)/6-311G**	51.5						
UMP4(SDQ)/6-31G*	48.4	60.3	11.9	56.9	64.8	7.9	−8.4
UMP4(SDQ)/6-311G**	43.4						
PUHF/6-31G*	6.8	15.0	8.2	−6.2	−2.5	3.8	13.0
PUHF/6-311G**	11.9						
PMP2/6-31G*	4.2	15.1	10.8	10.8	16.8	6.0	−6.6
PMP2/6-311G**	−0.9						
PMP3/6-31G*	15.0	25.5	10.5	17.2	22.9	5.8	−2.1
PMP3/6-311G**	11.2						
UB3-LYP/3-21G	16.1						
UB3-LYP/6-31G*	32.7	43.0	10.3	26.9	33.2	6.2	5.8
QCISD/6-31G*	32.3	42.9	10.6	38.3	44.7	6.5	−6.0
Experiment	29.7 ± 1.5						

[a] UHF/6-31G* geometries. [b] E_a for syndiotactic addition. [c] E_a for isotactic addition. [d] E_a(iso) − E_a(syn) [e] E_a(MAN) − E_a(AN).

Table 6.

(a) Contribution of Internal Rotations to Difference in A for AN and MAN (As Measured by $Q^\dagger/Q$ at 303 K)

	MAN			AN			
reactant/TS Mode	Q	$Q^\dagger$	$Q^{\dagger/Q}$	Q	$Q^\dagger$	$Q^{\dagger/Q}$	contribution to $A_{AN/AMAN}$[a]
free rot/τ_{TS1}	115	24.3	0.21	100	28.6	0.29	1.35
$\tau_{R1/\tau TS2}$	7.38	13.4	1.8	15.4	15.4	1.0	0.55
$\tau_{M1/\tau TS3}$	5.62	8.99	1.6				0.63
$\tau_{R2/\tau TS4}$	8.87	4.97	0.56				1.8

(b) Contribution to A of Transitional Modes Corresponding to Monomer External Rotations

	Q (monomer - ext rot)	$Q^\dagger$(3 transitional modes)	$Q^{\dagger/Q}$
MAN	8.26×10^4	238	2.89×10^{-3}
AN	2.60×10^4	338	1.30×10^{-2}
ratio MAN/AN	0.314	1.41	4.5

[a] $(Q^\dagger/Q)_{AN}/(Q^\dagger/Q)_{MAN}$ (for CH_3 rotations $(Q^\dagger/Q)_{AN} = 1.0$).

slope of an Arrhenius plot) are used to find the frequency factor in quantitative calculations, when examining trends it is helpful to use the *approximate* relation

$$A \approx \frac{k_B T}{h} \frac{Q^\dagger}{Q} \tag{5}$$

Since the low-frequency internal rotations significantly affect A, the contribution of these modes to $Q^\dagger/Q$ for each TS mode was calculated. The various components in this calculation are summarized in Table 6. It had been suggested[10,15] that methyl hindrance might explain the difference, and one might suppose that this could be because of the internal rotations that occur only in the methyl-substituted monomer. It could be that the CH_3 rotations in the radical and monomer would become more hindered (due to steric effects) as the reactants come together in the TS, decreasing A for the methyl-substituted monomer. However, the present calculations show that instead the monomer CH_3 rotation actually becomes less hindered: the partition function for this mode changes from 5.6 to 9.0 in going from reactants to TS, as seen in Table 6, while the radical CH_3 rotation becomes more hindered, as expected (the partition function for this mode changes from 8.9 to 5.0 in going from the reactants to the TS). This results in a cancellation of the effects of the two rotations. From Table 6, it can be calculated that the CH_3 rotations only account for a 12% increase in A for MAN relative to AN. In a similar calculation on τ_{TS1} (which corresponds to a monomer free rotation in the reactants), this mode was found to only cause a 35% increase in A for AN over MAN (Table 6).

Table 6 also shows that τ_{R1} and τ_{TS2} contribute to a 45% decrease in A for AN relative to MAN and therefore opposes the overall result that A for the methyl-substituted monomer is smaller than that for the unsubstituted monomer. Although both the τ_{R1} and τ_{TS2} rotations are more hindered in MAN (evident from the lower value of the partition function for the two modes in MAN, as seen in Table 6), the τ_{R1} rotation becomes significantly more hindered than the τ_{TS2} rotation. Since Q for MAN is much smaller than Q for AN, while $Q^\dagger$ is fairly similar for the two monomers, the net result is that $Q^\dagger/Q$ for the methyl rotation is larger for MAN than for AN.

Other low frequency modes which could significantly influence the difference in A for MAN and AN are the so-called *transitional modes* in the TS.[6,18] These modes correspond to three translational and three external rotational degrees of freedom in the reactants. The partition functions for these modes decrease dramatically in becoming hindered internal rotations and vibrations in the TS. Table 1 shows that there are four transitional modes under 200 cm^{-1}. Three of these (the τ_{TS1} internal rotation and two bending modes) approximately correspond to the three monomer external rotational degrees of freedom, while the fourth (a bending mode) corresponds to one of the monomer translational degrees of freedom. The transitional mode with an imaginary frequency is of course the reaction coordinate.

The contribution to A of the transitional modes corresponding to rotations (as measured by $Q^{\dagger}/Q$) is given in Table 6. The contribution from the transitional mode to the reactant partition function, Q_{TM}, is the external rotational partition function of monomer, while that for transition state, $Q_{TM}{}^{\dagger}$, was taken as the product of the partition functions of the three transitional modes (τ_{TS1} was treated as an internal rotation while the other two modes were treated as harmonic oscillators). Table 6 shows that Q_{TM} for AN is only 31% of Q_{TM} for MAN. This is almost entirely due to one of the principal moments of inertia of the MAN monomer being over 5 times that of the AN monomer (a direct result of the presence of the methyl group). On the other hand, the values of $Q_{TM}{}^{\dagger}$ for the two monomers are quite similar. In fact, $Q_{TM}{}^{\dagger}$ for AN is larger than $Q_{TM}{}^{\dagger}$ for MAN, opposite to what one would expect from the reduced moments of inertia or reduced masses for the two monomers. This result is due to the potential energy surfaces for these modes being much steeper (bending force constants much larger) in MAN than in AN. Since the only difference between the two monomers is the presence or absence of a methyl group, one can assume that the higher force constant for MAN is due to increased steric hindrance from the methyl groups. The effect of the higher force constant (which reduces $Q_{TM}{}^{\dagger}$) in MAN partially cancels with the effect of the higher reduced mass (which increases $Q_{TM}{}^{\dagger}$), the net result being that $Q_{TM}{}^{\dagger}$ for AN is larger than $Q_{TM}{}^{\dagger}$ for MAN. This cancellation does not occur for Q_{TM}, since the external rotations of the monomer are assumed to be free (rotational potential is zero everywhere, inherent in a gas-phase treatment), and so the only variable influencing Q_{TM} is the moment of inertia. The overall contribution to the difference in A (as measured by $Q^{\dagger}/Q$) from the rotational transitional modes (or the external rotations of the monomer) is a factor of 4.5 increase in A for AN over MAN, which accounts for almost all of the calculated difference in A (see Table 4).

It had been suggested[6,8,26] that the most important modes influencing differences in frequency factors are the three rotational transitional modes: two transitional modes corresponding to rotations in reactants (t_{TS1} and a bending mode), and τ_{TS2}. In actuality, it will now be shown that τ_{TS2} is unimportant in influencing differences in frequency factors, due to cancellation of its effects with the corresponding reactant mode τ_{R1} in the transition state expression; the other modes will however be seen to be influential.

The other TS modes under 200 cm^{-1} (see Table 1) also appear to make only a small contribution to the difference in A. $Q^{\dagger}/Q$ was calculated for all of the nontransitional and noninternal rotational TS modes under 200 cm^{-1} (based on the assignments in Table 1) assuming that they could all be treated as harmonic oscillators (since all of them are bending modes). It was found that overall the ratio $Q^{\dagger}/Q$ for these modes was only 8% larger for MAN than for AN.

For a pair of monomers with a much bulkier side chain than the CN group in MAN and AN, the difference in Q_{TM} would be much smaller, since the principal moments of inertia would not be significantly affected by the small methyl group. However, the reduced masses of the transitional modes would also be unaffected. Therefore, there would be no cancellation of the effect of the increase in force constant in the methyl-substituted monomer with any increase in reduced mass. One would then expect $Q_{TM}{}^{\dagger}$ for the methyl-substituted monomer to be significantly smaller than $Q_{TM}{}^{\dagger}$ for the unsubstituted monomer. The net result is that the difference in $Q^{\dagger}/Q$ for the pair of monomers with a bulky side chain would be similar in magnitude to the difference in $Q^{\dagger}/Q$ for MAN and AN. The contribution of the translational transitional modes would be smaller than that of the rotational transitional modes since the difference in Q_{trans} for AN and MAN (~30%) is much smaller than the difference in $Q_{ext\ rot}$. There is also only one translational transitional mode with a real frequency under 200 cm^{-1} which would have a major influence on $Q^{\dagger}$.

It can be concluded from this section that the difference between A's for methyl substituted and unsubstituted monomers is largely due to the difference in Q for the external rotational degrees of freedom of the monomer, combined with the similarity in $Q^{\dagger}$ for the corresponding rotational transitional modes in the TS. For MAN/AN, the difference in Q is a result of the large difference in one of the principal moments of inertia of the two monomers (because of the methyl group) while the similarity in $Q^{\dagger}$ is caused by a cancellation of the effects of an increase in the force constants (due to methyl hindrance) and an increase in the reduced mass for the modes in the methyl-substituted monomer. For monomers with bulky side chains, the difference in A probably arises from a corresponding difference in $Q^{\dagger}$ for the monomer pair (e.g., acrylate/methacrylate) because of different force constants, while the values of $Q_{ext\ rot}$ for the monomer pairs will be similar because of the similarity in moments of inertia.

Trends in Activation Energies. Table 5 shows that at most of the levels of theory used (including the highest—QCISD/6-31G*), the calculated E_a for AN is larger than that for MAN, opposite to the measured trend for BMA and BA. However, the levels of theory used are all below the minimum recommended to obtain accurate results (QCISD(T)/6-311G**)[8] (unfeasible with the computational resources available). There are no accurate Arrhenius parameters for k_p of acrylonitrile, although experiment suggests that it propagates up to 3 orders of magnitude faster than MAN at 25 °C.[37] However, AN does not swell its polymer, and hence polymerization mechanisms can be quite different, so equating these results to a lower E_a for AN is not reliable. Despite this, the importance of the factors that influence E_a may still be quantified using calculated geometries, which are not sensitive to the level of theory used. This analysis is now given.

The factors that have generally been invoked[38−42] to explain differences in E_a for radical reactions are (a) reaction enthalpy (strength of bonds formed/broken), (b) the degree of charge transfer in the transition state (polar factors), (c) steric repulsion in the transition state, and (d) resonance stabilization of the reactants relative to the transition state. There have been few accurate theoretical studies to quantify the contributions of the various factors to E_a in homopolymerization reactions. Most of the theories developed have been based on experimental data for radical reactions between very different substrates, which may overemphasize certain factors that may be unimportant in homopolymerizations. One problem with the analysis is that the small difference in E_a (5 kJ mol^{-1}—on the order of rotational barriers) makes it difficult to ascribe the difference unequivocally to any particular factor.

Reaction Enthalpy. The contribution of reaction enthalpy to E_a is really a combination of the other three factors, but applied to reactant and product rather than to the reactant and the transition state. Reaction enthalpy should be important if the TS is "productlike", i.e., if there is a significant energetic contribution to the TS from the energy of the forming and/or breaking bonds. Comparing the "monomer" double bond lengths (UHF/6-31G*) in the MAN and AN TSs (1.40 Å) to their lengths in the reactants (1.32 Å) and product radical (1.55 and 1.51 Å respectively), the TSs appear to be halfway between reactants and products. Furthermore, accurate theoretical values for reaction enthalpies and E_a are not available for comparison, making it difficult to determine the role of this factor.

Polar Factors. Polar stabilization of the TS occurs through mixing of charged configurations with the uncharged TS configuration, if the energy gap between configurations is small.[43−45] This results in a lowering of E_a and the development of a polar character in the TS. The Mulliken charges on the carbon atoms connecting the forming bond in the MAN and AN TSs are similar (−0.22 and −0.39 in the AN syndiotactic dimer TS and −0.06 and −0.39 in the MAN TS (UHF/6-31G*)), and the changes in charges from the reactants to the TS are almost identical. This suggests minimal polar effects.

There is also good experimental evidence for no significant effects from polar factors in homopolymerization reactions: the insensitivity of such reactions to solvent polarity[46] (excluding any effects of specific bonding of solvent with monomer[47−49]). For MAN,[9] there is no discernible difference in k_p in benzene (dielectric constant = 2.274 at 25 °C) and acetone (dielectric constant = 20.7).

From this accumulated evidence, it can be concluded that polar factors are probably not very important in explaining the trends in E_a.

Steric Factors. Steric factors include nonbonded interactions and angle strain (β-strain). The effect of nonbonded interactions was estimated using the Lennard−Jones (12,6) potential and literature values[50] for the Lennard−Jones well depth ϵ and diameter σ for CH_4, N_2 and H_2 (=137, 91.5 and 33.3 K and σ =3.82, 3.68 and 2.97 Å, respectively) for the $CH_3\cdots CH_3$, CN···CN, and H···H interactions, respectively. The applicability of any Lennard−Jones parameters for CN is however questionable due to the polarity of this group. $CH_3\cdots$CN, $CH_3\cdots$H, and CN···H interactions were calculated using the usual combining rules (geometric mean for ϵ, arithmetic mean for σ).

Table 7. Distances between Substituents (Å) in MAN and AN Syndiotactic Dimer TSs (Distances Measured from Carbon Atoms of Substituents for CH_3 and CN and from Hydrogen Atom for H)

interacting substituents	MAN	AN
CN−CN	4.31	4.25
CH_3−CN/H−CN	3.56	3.35
CH_3−CN/H−CN	3.51	3.31
CH_3−CH3/H−H	4.33	3.61

Table 8. Total Distortion Energies and Difference in Energies for MAN and AN (kJ mol^{-1}) in Propagation Reactions

level of theory[a]	MAN[b]	AN[b]	difference[c]
UHF	61.3	53.2	8.1
UMP2	26.8	22.7	4.1
PUHF	74.6	64.3	10.3
PMP2	38.1	32.2	5.9
UMP3	37.5	31.9	5.6
UMP4(D)	33.1	28.0	5.1
UMP4(DQ)	36.2	30.8	5.4
UMP4(SDQ)	36.4	30.6	5.8
PMP3	45.6	38.8	6.7
QCISD	41.4	34.8	6.6

[a] 6-31G* basis set. [b] Energy E ={E(monomer in TS geom.) + E(radical in TS geom)} − {E(monomer in reactant geom.) + E(radical in reactant geom.)}. [c] E(MAN) − E(AN).

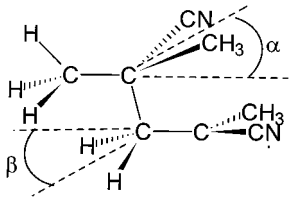

Figure 12. MAN TS illustrating angles α and β that define distortion from planarity in TS (angles measured between plane containing carbon atoms of substituents (or hydrogen atoms in case of H substituents) and polymer backbone carbon and line joining the two backbone carbons).

The nonbonded interactions were calculated by considering the pairwise interaction energies of the substituents (CH_3, CN, and H) in the MAN and AN TSs, measuring the distances from the carbon atoms of the substituents (in the case of CH_3 and CN) or from the hydrogen atom (in the case of H). These distances (for syndiotactic dimer TSs at UHF/6-31G* level of theory) are given in Table 7. The estimate of the difference in nonbonded interactions in the MAN TS and AN TS using this method is 3.9 kJ mol^{-1}.

The larger distortion from planarity of the monomer and radical in the formation of the TS for MAN is expressed in terms of the angles α and β in Figure 12; α is 36.8 and 33.3° in the MAN and AN TSs, respectively, while β is 27.6 and 25.0°, respectively. The values of α and β are zero in the reactants, indicating that β-strain may explain the difference in E_a.

The energy change for distortion of the monomer and monomer radical to their TS geometries was used as an estimate of β-strain (the geometry of a species in the TS was taken as the coordinates of the atoms belonging to that species in the TS). Bond lengths changes are similar in MAN and AN, so contributions from bond stretching can be ignored. The distortion energies were calculated at a number of levels of theory and are given in Table 8.

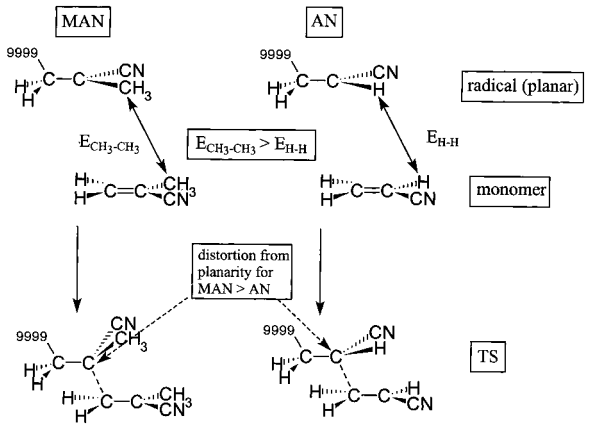

Figure 13. Illustration of difference in steric strain in the formation of the MAN and AN TSs.

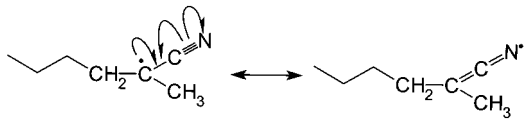

Figure 14. Resonance structures of MAN monomer radical.

The contribution of β-strain (~6 kJ mol^{-1}) is larger than the calculated nonbonded interactions at all levels of theory, but both effects are consistent with the observed difference in E_a for BMA and BA. The difference in β-strain for MAN and AN is also very similar at all levels of theory used, indicating that these energies due not suffer from the same problems as the E_a calculations and that they give good estimate of the true strain energy.

The difference in E_a is probably a combination of β-strain and nonbonded interactions. The geometry of the TS becomes distorted so as to move the substituents apart (to reduce nonbonded interactions), which in turn increases the angle strain. The final geometry minimizes the increase in energy due to the two factors. Since AN has no methyl groups, nonbonded interactions are smaller, resulting in less distortion in the TS and thus less angle strain. The differences in steric strain in the TSs of MAN and AN are illustrated in Figure 13. Steric factors, and β-strain in particular, may also be responsible for the differences in E_a found for the syndiotactic and isotactic TSs of both MAN and AN, since greater deviations from planarity are observed in the isotactic TS.

Resonance Stabilization. The shorter length of the C−C bond of the C−CN group in the MAN and AN monomer radicals (1.39 and 1.40 Å respectively) compared to a typical C−C single bond (1.54 Å) indicates extensive resonance stabilization is present (Figure 14). This is partially lost in the TS (the bond length increases to 1.44 and 1.45 Å respectively for MAN and AN) due to loss of planarity of the radical center. The larger distortion from planarity for MAN compared to AN should result in a larger loss of delocalization energy. The delocalization energy of the allyl radical of 119 kJ mol^{-1} (as reported by Mo *et al.*[51] using *ab intio* methods—see also comments by Gobbi and Frenking[52]), analogous to the C−C≡N delocalized system, shows that even a small difference in the loss of delocalization energy in the MAN and AN systems could have a significant effect on the difference in E_a (delocalization is not as extensive as one would expect for molecules with π-systems containing only carbon, since nitrogen is more electronegative than carbon, making the resonance hybrid on the right of Figure 14 less important than the one on the left).

It is noted that the angle-strain calculations carried out above do not separate delocalization from steric effects. The effect of delocalization on E_a being proposed here is not based mainly on the stability of the radical (which has been proposed previously[41]) but rather on the loss of this stability in the TS.

The role of hyperconjugation (due to the methyl substituents) does not appear to be significant, since the decrease in the C−CH$_3$ bond length and increase in the C−H bond lengths in CH$_3$ in the radical from their "typical" values expected with hyperconjugation[53] does not occur. This agrees with observations of changes in spin density in neutral radicals due to alkyl substituents by ESR spectroscopy, which show that the alkyl substituents only reduce the spin density on the central carbon atom by about 8%.[40]

The above arguments show that the difference in E_a for MAN and AN (and analogously between methacrylates and acrylates) can be explained entirely in terms of distortions from planarity in the TS, which are a combination of steric effects (angle strain and nonbonded interactions) and a loss of delocalization in the TS. While the effect of reaction enthalpy cannot entirely be discounted, since the TSs for propagation of both MAN and AN are intermediate between reactant and product, the origin of this enthalpic effect (or more precisely the difference in energy between reactant and product) would indeed the same as that discussed between reactant and transition state.

Similarities in Homologous Series

The similarity between frequency factors and activation energies for homopropagation in homologous series can be rationalized based on the results of the calculations given above.

It was concluded from the results in Figure 10 that steric hindrance to internal rotation is not affected very much by parts of the chain more than two carbon atoms from the axis of rotation. Since the substituents that differ in members of the homologous series that have been examined experimentally (e.g. the methacrylates) are more than two carbon atoms from the reacting centers, the hindrance to rotation and vibration of these substituents in the reactants and TS should be almost identical. Since the TS expression contains a ratio of the partition functions for the reactant and TS modes, there should be an almost exact cancellation of the effects of these modes. Thus A should be very similar for members of a homologous series. Similarly, the large distance from the reacting centers of these substituents results in a negligible electronic contribution to the TS from these groups (the alkyl chains also do not provide a favorable pathway for electron delocalization). Steric effects are also small due to the distance between the groups. Hence, E_a is similar for members of a homologous series.

Extant data for A and E_a for homologous series[11−14] do not appear to show any systematic trends: for example, the values of log A/dm^3 mol^{-1} s^{-1} for the series methyl, ethyl, and butyl methacrylates are 6.69, 6.65, and 6.68 respectively; those for E_a are 24.1, 23.9, and 23.6 kJ mol^{-1}. Any systematic differences in A for members of a homologous series may be due to the accumulation of small differences in the partition func-

tions of the low-frequency modes resulting from the presence of different substituents in the various monomers. As discussed before in the comparison of A for MAN and AN, even very slight systematic differences in the low frequencies can result in a significant effect on A. Any small differences in E_a for members of homologous series might be accounted for in terms of steric effects. In the comparison of MAN and AN, in which the substituents that differ in the two monomers are more closely separated in the TS, such effects amounted to a ~10 kJ mol^{-1} difference in E_a. The smaller difference in E_a for members of a homologous series merely reflects the greater separation in the TS of the substituents that differ in members of the homologous series.

Conclusions

At the highest level of theory used, the calculated frequency factor for propagation of MAN was found to be within a factor of 2 of the experimental value. The relatively small discrepancy between these values may be due to solvent effects, which were ignored in the calculations; these could cause the monomer rotations to be less free in the condensed phase than in the gas phase. Alternatively, the discrepancy may arise from the accumulation of small errors in the vibrational/hindered rotational function of many modes.[6] Because much of the ratio $Q^{\dagger}/Q$ comes from geometrical considerations which can be found to moderate accuracy with low levels of theory, frequency factors and rotational potentials were found as expected to be insensitive to the level of theory used (above the HF/3-21G level), although the semiempirical AM1 method does not perform very well. However, two of the internal rotations studied (one in the radical and one in the TS) were found to be sensitive to the chain length of the radical or TS used in the calculations. E_a is of course extremely sensitive to the level of theory used, and calculations at an adequate level (to an accuracy of, say, ±2 kJ mol^{-1}) were unfeasible.

On the basis of the comparison of transition state properties for propagation in the model systems of MAN and AN, it seems that the difference in A for propagation of acrylates and methacrylates is almost entirely due to hindrance caused by the methyl groups to the three transitional modes in the TS, which correspond to the three external rotational degrees of freedom of the monomer in the reactants (but not due to an increase in hindrance to methyl rotations in the TS of the methyl-substituted monomer). The difference in E_a for the same systems could be explained in terms of steric effects (angle strain/nonbonded interactions) and loss of delocalization in the TS. The difference in steric effects was quantified and found to agree with the measured difference in E_a. This analysis of differences in A and E_a can be applied to understanding trends in propagation in general.

Acknowledgment. The support of the Australian Research Council is gratefully acknowledged.

References and Notes

(1) Aleksandrov, H. P.; Genkin, V. N.; Kitai, M. S.; Smirovna, J. M.; Sokolov, V. V. *Kvantovaya Elektron. (Moscow)* **1977**, *4*, 976.
(2) Olaj, O. F.; Bitai, I. *Angew. Makromol. Chem.* **1987**, *155*, 177.
(3) Buback, M.; Garcia-Rubio, L. H.; Gilbert, R. G.; Napper, D. H.; Guillot, J.; Hamielec, A. E.; Hill, D.; O'Driscoll, K. F.; Olaj, O. F.; Shen, J.; Solomon, D.; Moad, G.; Stickler, M.; Tirrell, M.; Winnik, M. A. *J. Polym. Sci., Polym. Lett. Ed.* **1988**, *26*, 293.
(4) Beuermann, S.; Buback, M.; Gilbert, R. G.; Hutchinson, R. A.; Klumpermann, B.; Olaj, F. O.; Russell, G. T.; Schweer, J. *Macromol. Chem. Phys.* **1997**, *198*, 1545.
(5) Buback, M.; Gilbert, R. G.; Hutchinson, R. A.; Klumperman, B.; Kuchta, F.-D.; Manders, B. G.; O'Driscoll, K. F.; Russell, G. T.; Schweer, J. *Macromol. Chem. Phys.* **1995**, *196*, 3267.
(6) Heuts, J. P. A.; Radom, L.; Gilbert, R. G. *Macromolecules* **1995**, *28*, 8771.
(7) Heuts, J. P. A.; Gilbert, R. G.; Radom, L. *J. Phys. Chem.* **1996**, *100*, 18997.
(8) Heuts, J. P. A.; Sudarko; Gilbert, R. G. *Macromol. Symp.* **1996**, *111*, 147.
(9) Shipp, D. A.; Smith, T. A.; Solomon, D. H.; Moad, G. *Macromol. Rapid Commun.* **1995**, *16*, 837.
(10) Lyons, R. A.; Hutovic, J.; Piton, M. C.; Christie, D. I.; Clay, P. A.; Manders, B. G.; Kable, S. H.; Gilbert, R. G. *Macromolecules* **1996**, *29*, 1918.
(11) Hutchinson, R. A.; Beuermann, S.; Paquet, D. A.; McMinn, J. H. *Macromolecules* **1997**, *30*, 3490.
(12) Beuermann, S.; Paquet, D. A.; McMinn, J. H.; Hutchinson, R. A. *Macromolecules* **1996**, *29*, 4206.
(13) Hutchinson, R. A.; Paquet, D. A.; McMinn, J. H.; Fuller, R. E. *Macromolecules* **1995**, *28*, 4023.
(14) Zammit, M. D.; Coote, M. L.; Davis, T. P.; Willett, G. D. *Macromolecules* **1998**, *31*, 955.
(15) Balic, R.; Gilbert, R. G.; Zammit, M. D.; Davis, T. P.; Miller, C. M. *Macromolecules* **1997**, *30*, 3775.
(16) Hutchinson, R. A.; Richards, J. R.; Aronson, M. T. *Macromolecules* **1994**, *27*, 4530.
(17) Hutchinson, R. A.; Paquet, D. A.; McMinn, J. H.; Beuermann, S.; Fuller, R. E.; Jackson, C. *DECHEMA Monogr.* **1995**, *131*, 467.
(18) Gilbert, R. G.; Smith, S. C. *Theory of Unimolecular and Recombination Reactions*; Blackwell Scientific: Oxford, England, and Cambridge, MA, 1990.
(19) Truhlar, D. G.; Garrett, B. C.; Klippenstein, S. J. *J. Phys. Chem.* **1996**, *100*, 12771.
(20) Voth, G. A.; Hochstrasser, R. M. *J. Phys. Chem.* **1996**, *100*, 13034.
(21) Chapman, S.; Hornstein, S. M.; Miller, W. H. *J. Am. Chem. Soc.* **1975**, *97*, 892.
(22) Hynes, J. T. *Annu. Rev. Phys. Chem.* **1985**, *36*, 573.
(23) Hehre, W. J.; Radom, L.; Schleyer, P. v. R.; Pople, J. A. *Ab Initio Molecular Orbital Theory*; Wiley: New York, 1986.
(24) Scott, A. P.; Radom, L. *J. Phys. Chem.* **1996**, *100*, 16502.
(25) Frisch, M. J.; Trucks, G. W.; Schlegel, H. B.; Gill, P. M. W.; Johnson, B. G.; Robb, M. A.; Cheeseman, J. R.; Keith, T.; Petersson, G. A.; Montgomery, J. A.; Raghavachari, K.; Al-Laham, M. A.; Zakrzewski, V. G.; Ortiz, J. V.; Foresman, J. B.; Peng, C. Y.; Ayala, P. Y.; Chen, W.; Wong, M. W.; Andres, J. W.; Replogle, E. S.; Gomperts, R.; Martin, R. L.; Fox, D. J.; Binkley, J. S.; Defrees, D. J.; Baker, J.; Stewart, J. P.; Head-Gordon, M.; Gonzalez, C.; Pople, J. A. GAUSSIAN 94 (Revision B.3), Pittsburgh, PA, 1995.
(26) Heuts, J. P. A.; Gilbert, R. G.; Maxwell, I. A. *Macromolecules* **1997**, *30*, 726.
(27) Aleman, C.; Julia, L. *J. Phys. Chem.* **1996**, *100*, 1524.
(28) Coussens, B.; Pierloot, K.; Meier, R. J. *J. Mol. Struct.: THEOCHEM* **1992**, *259*, 331.
(29) Fabian, W. M. F. *J. Comput. Chem.* **1988**, *9*, 369.
(30) van Herk, A. M. *J. Chem. Educ.* **1995**, *72*, 138.
(31) Baskin, J. S.; Gupta, M.; Chachisvilis, M.; Zewail, A. H. *Chem. Phys. Lett.* **1997**, *275*, 437.
(32) McCaskill, J. S.; Gilbert, R. G. *Chem. Phys.* **1979**, *44*, 389.
(33) Wong, M. W.; Radom, L. *J. Phys. Chem.* **1995**, *99*, 8582.
(34) Tozer, D. J.; Handy, N. C.; Amos, R. D.; Pople, J. A.; Nobes, R. H.; Xie, Y.; Schaefer, H. F. *Mol. Phys.* **1993**, *79*, 777.
(35) Chen, W.; Schlegel, H. B. *J. Chem. Phys.* **1994**, *101*, 5956.
(36) Stanton, J. F. *J. Chem. Phys.* **1994**, *101*, 371.
(37) Brandrup, A.; Immergut, E. H. In *Polymer Handbook*, 3rd ed.; Brandrup, A., Immergut, E. H., Eds.; Wiley-Interscience: New York, 1989.
(38) Tedder, J. M. *Angew. Chem., Int. Ed. Engl.* **1982**, *21*, 401.
(39) Giese, B. *Angew. Chem., Int. Ed. Engl.* **1983**, *22*, 753.
(40) Rüchardt, C. *Angew. Chem., Int. Ed. Engl.* **1970**, *9*, 830.
(41) Bamford, C. H. In *Comprenhesive Polymer Science*; Allen, G., Bevington, J. C., Eds.; Pergamon: Oxford, England, 1989; Vol. 3, p 219.

(42) Moad, G.; Solomon, D. H. *The Chemistry of Free Radical Polymerization*; Pergamon: Oxford, England, 1995.
(43) Wong, M. W.; Pross, A.; Radom, L. *J. Am. Chem. Soc.* **1993**, *115*, 11050.
(44) Wong, M. W.; Pross, A.; Radom, L. *J. Am. Chem. Soc.* **1994**, *116*, 6284.
(45) Wong, M. W.; Pross, A.; Radom, L. *J. Am. Chem. Soc.* **1994**, *116*, 11938.
(46) Reichardt, C. *Solvents and Solvent Effects in Organic Chemistry*; 2nd ed. ed.; Verlag Chemie: Weinheim, Germany, New York, 1988.
(47) O'Driscoll, K. F.; Monteiro, M. J.; Klumperman, B. *J. Polym. Sci., Part A: Polym. Chem.* **1997**, *35*, 515.
(48) Zammit, M. D.; Davis, T. P.; Willett, G. D.; O'Driscoll, K. F. *J. Polym. Sci., Part A: Polym. Chem.* **1997**, *35*, 2311.
(49) Olaj, O. F.; Schnöll-Bitai, I. *Eur. Polym. J.* **1989**, *25*, 635.
(50) Hirschfelder, J. O.; Curtiss, C. F.; Bird, R. B. *Molecular Theory of Gases and Liquids*; Wiley: New York, 1964.
(51) Mo, Y. R.; Lin, Z. Y.; Wu, W.; Zhang, Q. N. *J. Phys. Chem.* **1996**, *100*, 6469.
(52) Gobbi, A.; Frenking, G. *J. Am. Chem. Soc.* **1994**, *116*, 9275.
(53) Gault, J. W.; Glukhovysev, M. N.; Radom, L. *Chem. Phys. Lett.* **1996**, *262*, 187.

MA980229N